DEVELOPMENT OF RHEOLOGICAL MEASUREMENT METHOD FOR FRESH CONCRETE CONSIDERING ITS GRANULAR CHARACTERISTIC

Zhuguo Li[1], and Minoru Iidaka[2]

[1.] Professor, Yamaguchi University, li@yamaguchi-u.ac.jp
[2.] Technical staff, Tsukuba University, iidaka@sie.tsukuba.ac.jp

ABSTRACT

In this paper, the author introduced a new rheological model of fresh concrete, briefly called VGM (Viscous Granular Material) model, which can exactly describe the rheological behaviors of fresh concrete before and after yield, including nonlinear flow, pressure and stress duration–dependence, and dilatant flow, etc. For measuring the parameters in the VGM model, a ring shear apparatus, named RSNS rheometer, was developed. The RSNS rheometer can measure the rheological performances of fresh concrete under a desired normal stress by either the stress-controlled method or the shear strain rate-controlled method. Measurement methods of the rheological parameters were discussed in detail based on the RSNS rheometer. Finally, an experiment was performed to investigate the variation of the rheological parameters of high fluidity concrete with the elapsed standing time. As a result, with the increase of the standing time of fresh concrete sample, the parameter τ_f, ϕ, θ_f, $\dot{\gamma}_t$, c_2/c_6 and c_3/c_6 become large, but the γ_f almost does not change, and the c_8 decreases. Moreover, the η and the C_{w1} increased with the elapsed standing time, but they decrease on the contrary if the elapsed time is too long. The time-dependence of the κ is opposite to the η and the C_{w1}.

Keywords: fresh concrete, rheometer, granular feature, vertical pressure, stress–controlled test, rheological model

---

Zhugou Li, Professor, PhD
Yamaguchi University
2-16-1 Tokiwadai, Ube, Yamaguchi, 755-8611, Japan

Email: li@yamaguchi-u.ac.jp
Tel: +81 836 85 9731

1. INTRODUCTION

Fresh concrete is solid-like material to liquid-like material from dry mixture to high fluidity mixture. But it is not a solid or a fluid because it can deform largely even 0-slump mixture and it is a granular with internal friction. The deformation and flow behaviors are complicated, being nonlinear, thixotropic, pressure-dependent and dilatancy. However, since Tattersall [1] proposed the Two-point Workability Test in 1973, fresh concrete is generally regarded as a viscous fluid, of which the relationship between shear stress and shear rate is linear, so-called Bingham model with two constants-yield stress and plastic viscosity. The Bingham model can not accurately and fully evaluate these complicated characteristics. It is also difficult to reappear the deformation and flow of fresh concrete by numerical simulation with Bingham model.

In order to describe the nonlinear, thixotropic, pressure-dependent and dilatant properties of fresh concrete's rheological behaviors, several modified Bingham models were proposed [2, 3, 4]. However, these models only considered a single property and lacked theoretical ground, and their validities have not been verified. Moreover, except yield stress and plastic viscosity, other parameters in the modified Bingham models have no definite physical meanings, and their measurement methods have not been proposed.

On the other hand, up till now, there are many rheometers proposed to measure the Bingham constants, e.g. yield stress and plastic viscosity, such as Coaxial Cylinder Rheometer (BML [5]), Parallel Plate Rheometer (BTRHEOM [6]), Impellers Rheometer (IBB [7], Two-Point Rheometer [8]), Vane-In Cup Rheometer (ICAR rheometer [9]) and shear box [2, 10, 11]. Compared with the slump test, the Bingham constants measured by these rheometers can describe not only the yield stress, but also evaluate viscous feature of fresh concrete. However, these rheometers have at least five problems: 1) Because these rheometers generally adopt rotational speed-controlled method, yield stress is determined by a linear regression analysis of shear stress-shear rate relationship rather than a direct measurement. 2) Shear deformation behavior before yielded can not be evaluated. 3) Fresh concrete's deformation and flow depends on vertical pressure on the shear plane so that the measured Bingham constants is related to sample thickness, but the sample size of these rheometers are different, and the normal stress on the shear plane is not clear. 4) These rheometers are designed based on Bingham model so that the nonlinear feature of fresh concrete can not be evaluated and the rheological parameters other than the Bingham constants can not be measured. 5) The rheometers that adopt rotational speed-controlled method only evaluate the rheological behaviors of fresh concrete under compulsory deformation and flow, whereas fresh concrete deforms or flows freely under a force, such as gravity, pump pressure, and vibration force, during construction process.

Li et al. proposed a multiphase model (particle assembly containing water) of fresh cementitious materials, and developed a microscopic approach to clarify theoretically the rheological properties of cementitious material [12, 13]. Moreover, Li et al. [14] fabricated a shear box, which has both stress control and shear rate control functions, to investigate the free and small deformation behavior of fresh concrete under shear stress by using stress control method, and the shear resistance of fresh concrete under compulsory shear deformation by using shear rate control method. Based on the theoretical analysis [15] and the experimental investigations [14, 16], Li [17] proposed a mechanical constitutive model for describing the shear deformation and flow behaviors of fresh concrete from small deformation to high-speed flow, which is called briefly VGM (Viscous Granular Material) model here, and gave the test methods for the parameters in the VGM model by developing a ring shear apparatus with load control and rotational speed control functions. The VGM model can describe the nonlinear, thixotropic, pressure-dependent and dilatancy characteristics of fresh concrete. This paper introduces the VGM model and the rheological test method, and the time-dependence of rheological properties of fresh concrete is discussed, using this ring shear type rheometer.

2. RHEOLOGICAL MODEL OF FRESH CONCRETE

2.1. Shear deformation model before yield

According to the past study [15], with the advance of shear stress, shear deformation firstly occurs in fresh concrete. If shear stress exceeds the shear failure limit stress (apparent yield stress), fresh concrete is yielded and shear flow happens. The shear deformation model of fresh concrete before yield is expressed as Eq. (1).

$$\gamma = \frac{c_6 \cdot \tau}{c_2 + c_3\tau} \cdot \frac{1}{\sigma_n + C_{w2}} \cdot [1 - \exp(-qt)] = \gamma_\infty \cdot [1 - \exp(-qt)] \quad (\tau \le \tau_f,\ \gamma \le \gamma_f,\ t \le t_f) \tag{1}$$

where, τ is shear stress, τ_f is shear failure limit stress, t is load lasting time, t_f is loading time till the yield point, γ is shear strain, γ_f is shear strain at shear failure point, ϕ is mean inter-particle frictional angle, θ is particle contact angle, θ_0, θ_f is average particle contact angle at the initial state, and the shear failure point, respectively, C_{w2}, f_{wm} is shear resistance, and adhesive force caused by the surface tension and suction of mixing water, respectively, σ_n is normal stress on the shear plane, N is amount of particle contact points on unit area of the shear plane, and Λ_0 is average particle moving distance in the beginning of loading.

$$c_2 = \phi + \theta_0, \qquad q = c_8(\sigma_n + C_{w2})\left(\frac{c_2 + c_3\tau}{c_6}\right)^2$$

$$c_3 = \frac{\theta_f - \theta_0}{\tau_f}, \qquad C_{w2} = N f_{wm} \cos\theta,$$

$$c_6 = \frac{1}{2} N \Lambda_0, \qquad \gamma_\infty = \frac{c_6 \cdot \tau}{c_2 + c_3\tau} \cdot \frac{1}{\sigma_n + C_{w2}}$$

Eq. (1) indicates that the shear strain (γ) increases with the increase of shear stress, and γ under a certain shear stress increases from zero to the maximum value (γ_∞) with time. If shear load is applied in a certain loading speed (s_1), $\dot{\gamma}$ is measured by stress control method, the equation of shear strain rate before yield is expressed by Eq. (2)

$$\dot{\gamma} = \frac{c_2 c_6 s_1 / (\sigma_n + C_{w2})}{(c_2 + c_3\tau)^2}\left[1 - \exp\left(-q\frac{\tau}{s_1}\right)\right] + \frac{c_7\tau(c_2 + 3c_3\tau)}{\exp(q\tau / s_1)} \tag{2}$$

where $\dot{\gamma}$ is shear strain rate, and s_1 is loading speed during stress-controlled test.

With the increase of shear stress, although the first term of right side of Eq. (2) increases, the second term tends to decrease when the shear stress exceeds a certain value. Hence, with the growth of τ, the $\dot{\gamma}$ before yield increases in the beginning, but inversely decreases if it reaches to a certain value, and the $\dot{\gamma}$ is close to zero at the shear failure point. The increasing phenomenon of $\dot{\gamma}$ is a response to an external force in the suspension state, at which the contact of particle is not close so that some solid particles are in a suspension state, whereas in the decrease stage of $\dot{\gamma}$, fresh concrete is in a visco-elastic-plastic state.

2.2. Shear deformation resistance model after yield

The particle in fresh concrete moves when the inter-particle force is larger than the resistance caused by the particle moving resistance angle (summation of inter-particle frictional angle and particle contact angle). Before yield, part of particles (called moving particle) move to their stable positions where inter-particle forces can be supported, their mean particle contact angle increases, thus the particle interlocking becomes strong. However, the increase of each particle contact angle has a limit. If the limit is exceeded, the particle can not go to a stable position and it continues to move, its

particle contact angle decreases, which is called failure particle. Fresh concrete sample is yielded and comes into shear failure state when failure particle occurs. In the shear failure state, average particle contact angle decreases and particle interlocking becomes weak.

The shear stress at the shear failure point, i.e. shear failure limit stress is expressed by Eq. (3) [15].

$$\tau_f = \sigma_n \tan(\theta_f + \phi) + C_{w1} \tag{3}$$

where C_{w1} is shear resistance caused by the surface tension and suction of mixing water.

Based on a series of theoretical analyses [15, 17], the shear flow resistance model after yield is expressed as Eq. (4).

$$\begin{aligned} \tau &= \sigma_n \tan\left[\theta_f e^{-\kappa\cdot\dot{\gamma}\cdot(t-t_f)} + \phi\right] + C_{w1} + \frac{\eta}{\cos[\theta_f e^{-\kappa\dot{\gamma}(t-t_f)}]}\dot{\gamma} \\ &= \tau_f^* + \eta_a\dot{\gamma} \qquad (\tau > \tau_f, \gamma > \gamma_f, t > t_f) \end{aligned} \tag{4}$$

where, η is the viscosity, called essential viscosity here, which is associated with temperature and potential energy of cement particles when there is no particle contact in fresh concrete, κ is a constant related to the time-dependence, τ_f* is apparent yield stress, and η_a is apparent plastic viscosity.

$$\eta = \frac{\cos\theta_f NH\exp(E/kT)}{\Lambda_0\Lambda_c N_c}, \tag{5}$$

$$\eta_a = \eta / \cos[\theta_f e^{-\kappa\dot{\gamma}(t-t_f)}] \tag{6}$$

$$\tau_f^* = \sigma_n \tan\left[\theta_f e^{-\kappa\cdot\dot{\gamma}\cdot(t-t_f)} + \phi\right] + C_{w1}$$

where, E is mean potential energy of cement particles that creates a viscous resistance to cement particle movement, T is absolute degree, H is Planck constant, Λ_c is average moving distance of cement particles, and N_c is number of cement particles.

The coefficient of shear strain rate term in Eq.(4), i.e. apparent viscosity η_a becomes small and approaches to the essential viscosity η with the increase of deformation after yield. Due to the introduction of normal stress σ_n, and loading time t in Eq.(4), the apparent yield stress τ_f* changes with loading time and normal stress, and the apparent viscosity η_a varies with loading time. Thus, Eq.(4) can simultaneously describe the nonlinear feature, pressure-dependence, and thixotropy of flow behavior after yield.

Based on Eqs. (1), (2) and (4), the conceptual diagrams of shear deformation and shear flow resistance of fresh concrete are shown in Figure 1. As shown in Figure 1(a), the shear strain (γ) of fresh concrete increases with the

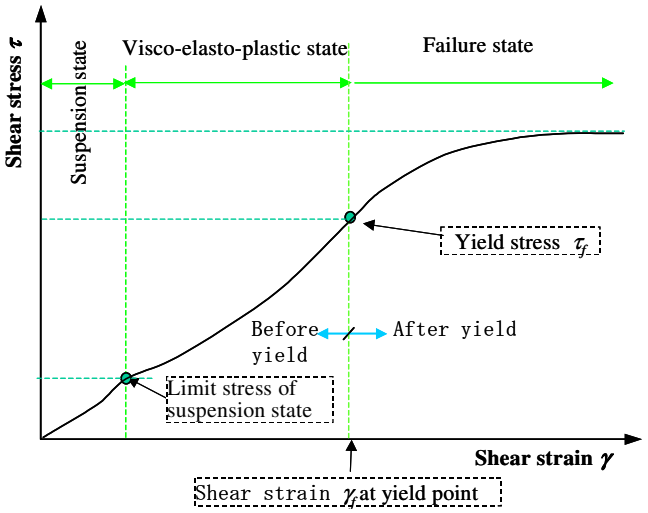

(a) Shear deformation model under an increasing shear tress

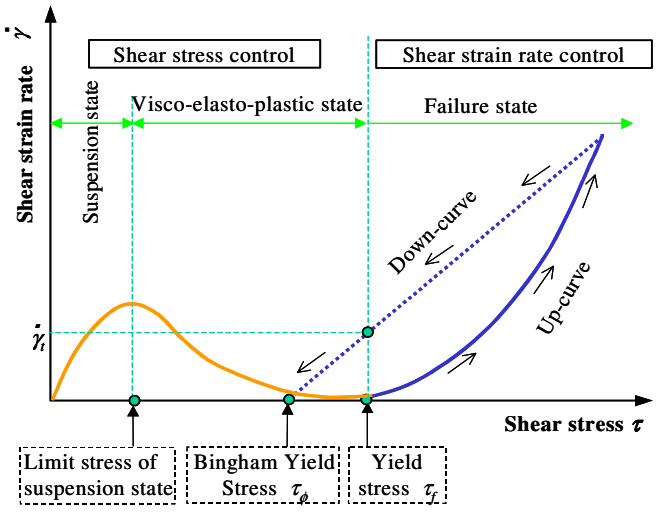

(b) Shear flow resistance model

Figure 1. Deformation and flow resistance models of fresh concrete

increase in shear stress, but when it reaches to the shear failure limit strain γ_f, fresh concrete is yielded and enters into the failure state. For non-viscous granular materials such as sand, the shear stress decreases with the decrease in mean particle contact angle in shear failure state. However, for viscous granular materials like fresh concrete, since the shear deformation accelerates in the failure state, the viscous resistance increases due to the rising of shear rate, the shear stress after yield does not decrease.

On the other hand, as shown in Figure 1(b), in case of shear rate control test, with the growth of $\dot{\gamma}$, τ increases after yield (see the up-curve of flow curve), but the τ- $\dot{\gamma}$ relationship is nonlinear. After reaching to a certain shear strain rate, if reducing $\dot{\gamma}$, τ decreases accordingly, but the down-curve is in the left of the up-curve, i.e., the τ in the down-curve is smaller than that in the up-curve for the same $\dot{\gamma}$. Generally, it is called thixotropy that the up-curve and down-curve of flow curve are not repeated. Thixotropy is caused by particle flocculation and dispersion, which has large effect on the shear flow resistance. In the equations of τ_f*and η_a, loading time is taken as a variable as shown in Eqs.(5) and (6), the τ_f*and η_a decrease with the loading time. Thus, Eq.(4) can describe the thixotropic characteristic of fresh concrete.

In the shear failure state, since the number of failure particles increases with shear flow, average particle contact angle continues decreasing. If a certain deformation ($=\dot{\gamma}(t - t_f)$) reaches, θ ($=\theta_f \cdot e^{-\kappa\dot{\gamma}(t-tf)}$) is close to zero, and thus the Eq. (4) of shear flow resistance can be changed into Eq. (7). The τ- $\dot{\gamma}$ relationship is linear, and the down-curve of flow curve is a straight line.

$$\tau = \tau_\phi + \eta\dot{\gamma}, \quad \tau_\phi = \sigma_n \tan\phi + C_{w1} \tag{7}$$

where, τ_ϕ is Bingham yield stress.

The yield stress (τ_ϕ) and plastic viscosity (Bingham constants), which can be obtained from the approximate straight line of the down-curve, can characterize the shear resistance caused by inter-particle friction and adhesive force of mixing water, and essential viscosity η, respectively. η is independent on the particle arrangement and can reflect the fluid feature of fresh concrete. However, the τ_f, as shown in Eq.(3), contains the resistance due to particle arrangement besides inter-particle friction and adhesive force of mixing water, thus it can well describe the granular characteristic of fresh concrete. The pressure-dependence of rheological property is caused by the inter-particle friction and the particle arrangement, the normal stress σ_n is included into τ_f*and τ_f, as shown in Eqs.(3) and (6). Thus, the VGM model can describe the pressure-dependence of rheological property of fresh concrete.

3. RING SHEAR TYPE RHEOMETER

3.1. Device

The BTRHEOM rheometer [18] may be sorted as a parallel plate rheometer, but there is no plate applying shear stress to concrete except for the blades. It is reported that the BTRHOEM rheometer is applied to the measurement of the Bingham constants of the fresh concrete with slump of 8~29cm (slump flow: 75cm) [18, 19], but not to the fresh concrete with slump under 8 cm since it is difficult to regard it as a Bingham fluid. In order to verify the reliability of BTRHOEM rheometer, Hu et.al compared the measured results of BTRHEOM rheometer with the numerical results of Finite Element Method (FEM) and the measured results of other rheometers (CEMAGREF-IMG and LAFARGE rheometers). In case of yield stress, there was not obvious difference between the measured result of BTRHEOM rheometer and numerical result. However, the measured result of plastic viscosity was 10% larger than the numerical result. And when segregation does not happen, the measured results of yield stress and plastic viscosity of BTRHEOM rheometer were almost the same as those of CEMAFREF-IMG rheometer and were closely related to those measured by the LAFARGE rheometer [18]. However, the BTRHEOM rheometer was designed to measure the Bingham constants,

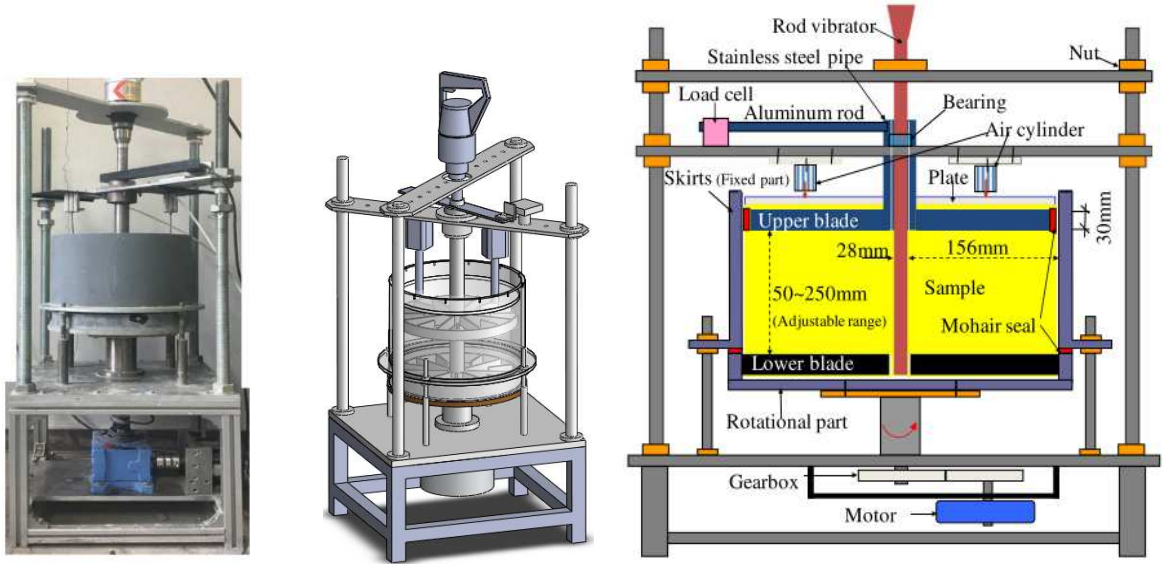

(a) Photograph of rheometer (b) Three denmensional image (c) Geometry

Figure 2. RSNS rheometer

it adopts rotational speed control method and the rotational speed is above 0.2 rev/s. Also, the effect of vertical pressure on flow resistance cannot be evaluated.

Since ring shear test has the advantages that the mechanical behaviors under continuous and large deformation can be measured and the normal stress on shear plane can be adjusted. It is widely used in mechanical test of soil and sand, and was already standardized (ASTM D7608-10, ASTM D6467-13). The BTRHEOM rheometer is also sorted as ring shear test method.

In our study, referring to the BTRHEOM rheometer, a ring shear apparatus was developed, which can measure the small deformation behavior under shear stress control, and the high-speed deformation (flow) behavior under rotational speed control. And the normal stress on shear plane can be adjusted by two air cylinders. For adding vertical pressure, the upper blade is fixed, whereas the lower blade is rotated, differentiating from the BTRHEOM rheometer. This shear apparatus is called RSNS (Ring Shear under adjusted Normal Stress) rheometer, as show in Figure 2 [17].

According to the maximum size of aggregate, the distance between the two blades can be adjusted up to 250mm. The lower blade and lower skirt are connected and rotate simultaneously by driving of a motor. The mohair seal was stuck on the edge of lower skirt to prevent concrete sample from escaping through the 3 mm gap between the upper and lower PVC skirts. For filling densely concrete sample into the container by vibration, and making a static center axis of ring shear, a rod vibrator with diameter of 28 mm is inserted into the center of two blades, but does not contact the bottom of the lower skirt. Also, to prevent the rod vibrator from rotating, the rod vibrator is fixed on the upper horizontal plate.

The sample is filled into the container up to 20mm higher than the top surface of the upper blade. After filling concrete sample by vibration, the height of sample is measured. Two air cylinders are met on the round aluminum plate locating on the concrete sample. The air cylinders are connected to a compressor, the vertical pressure applied to concrete sample is adjusted by the air pressure of cylinder.

The RSNS rheometer has functions of both the torque control and angular velocity control. Firstly, the rotational angle is measured under the torque control method, in which torque increases from zero. Once the shear stress exceeds yield stress τ_f, concrete sample enters into the failure state, then the RSNS rheometer automatically changes into the angular velocity control method. The torque is measured when rotational speed increased or decreased.

Because there are friction resistance and adhesive resistance at the inside wall of container and the surface of vibrator as well as concrete inside's shear resistance, part of the torque applied to concrete

sample by the lower blade was consumed by these resistances, the torque of the upper blade, measured by a load cell, is smaller than that of the lower blade. Only when the upper torque is over zero, it is judged that whole sample is in shear state. According to the investigation of test accuracy of the BTRHEOM rheometer, the friction resistance and adhesive resistance do not have obvious effect. And for the RSNS rheometer, the radius (156 mm) of sample was larger than that of BTRHEOM rheometer, the effects of friction resistance and adhesive resistance at the inside wall of container and the surface of vibrator are further reduced. Hence, the lower blade torque (motor's torque minus self-resistance of apparatus) is used to calculate the shear stress acting on the bottom of concrete sample.

Shear deformation and dilatancy simultaneously occurs in fresh concrete, but the shape of the upper blade allows concrete sample to expand or shrink. Hence, the shear thickness of concrete sample does not change even though dilatancy happens.

Average shear strain (γ_m) and average strain rate ($\dot{\gamma}_m$) of ring shear are in the middle position between the container and the rod vibrator, and described by Eq.(8). And the shear stress (τ_m) in the middle position is shown in Eq.(9) [17].

$$\gamma_m = \frac{\pi(R_1 + R_2)\varphi}{360h}, \quad \dot{\gamma}_m = \frac{\pi(R_1 + R_2)\Omega}{360h} \tag{8}$$

$$\tau_m = \frac{3\Gamma_m}{2\pi(R_2^3 - R_1^3)} \tag{9}$$

where, R_1 and R_2 are respectively the radius of central axis and container, h is thickness of sample between two blades, φ is rotational angle of the lower blade, Ω : is rotational angle speed of the lower blade, and Γ_m is toque applied to concrete sample by the lower blade.

In this study, we used the RSNS rheometer to evaluate the rheological property of fresh concrete by measuring the relationships between mean shear strain and shear stress before yield and between mean shear strain rate and shear stress. If fresh concrete follows the Bingham model, mean shear stain /rate and mean shear stress occur at the same place where is the middle position between the container and the rod vibrator. However, for nonlinear material, the positions of mean shear stress and mean shear strain rate are different. Moreover, because the ring shear strain of the outermost part of sample is largest, the shear stress should also be largest there. Hence, for a granular material, the shear failure begins firstly at the outermost part, and then advances inside (progressive failure) [20]. The shear stress of the outermost sample at shear failure point is equal to yield stress. The average shear stress must be smaller than the outermost shear stress. Also, the shear strain at position of the average shear stress is not equal to the average shear strain. Therefore, an error would be caused in the test result of rheological parameters gotten in the latter based on the τ_m-γ_m, τ_m-$\dot{\gamma}_m$ relationships. However, in the case of fresh concrete, particles' moving distances in circumference are coordinated because strong particle interlocking results in a large inter-particle's drawing. Hence, it is possible that the mean shear stress and the mean shear strain occur at the same position, and the test error is not so great. Quantitative evaluation on the test error is a future work.

On the other hand, the normal stress is approximately calculated by Eq. (10) [17].

$$\sigma_n = 9.8 \cdot (h_t + \frac{h}{2})\rho + \frac{m_a + 2PA_c}{\pi(R_2^2 - R_1^2)} \tag{10}$$

where h_t is sample thickness from the bottom of the upper blade to the surface of sample, ρ is density of concrete sample, m_a is mass of round aluminum plate, A_c is section area of one air cylinder, and P is output pressure of air cylinder.

3.2. Test method of rheological parameters

Based on a series of theoretical analyses [17], measuring procedure and calculating methods of the parameters in the VGM model were proposed as follows:

Step 1: Constant torque stage. The input value of motor's torque is set, a small and constant torque acts on the sample by the lower blade, the torque of the upper blade is detected by the load cell, and rotational angle of the lower blade under the constant torque is recorded. The set of motor's torque is done by trail and error, which is small as possible, but it should ensure that the torque of the upper blade, detected by the loading cell, is within 1.0~3.0 N·m and the rotational speed of lower blade is within 0.5~1.5 deg./s.

Step 2: Torque growth stage. The output torque of motor is increased under a small increasing speed. The output torque and the rotational angle of the lower blade are recorded. Once the sample enters into the shear failure state, the rotational speed increases rapidly and exceeds 5 deg./s, this torque increasing stage automatic ends. The measurement in the above two stages is done under no external pressure of the air cylinders.

Base on the experimental results of the torque increasing state, shear stress τ_m, average strain γ_m and average strain rate $\dot{\gamma}_m$ are calculated according to Eqs. (8), (9), respectively. The τ_m- γ_m and τ_m- $\dot{\gamma}_m$ relationships are plotted, shear failure limit stress τ_f and the corresponding shear strain γ_f are decided. And the relational curve (straight line) of $(\tau_m/\sigma_n)/\dot{\gamma}_m-\tau$ is drawn, the slope of the line is c_3/c_6 and the intercept is c_2/c_6 in Eq.(1). Finally, based on the experimental results of the constant torque stage, the relational curve (straight line) of $\ln(-\ln(\gamma_m/\gamma_{m\infty}))$-$t$ is drawn. The absolute value of the right line's slope is q. Using the values of τ, σ_n, c_2/c_6 and c_3/c_6, the value of c_8 is further obtained.

Step 3: Constant rotational speed stage. The rotational angular speed of motor is set to be a certain value and less than 5 deg./s. When the motor torque decreases gradually with the rotational displacement of sample and approaches to a constant, the measure is shifted to Step 4.

Step 4: Rotational speed growth stage. The rotational angular speed is increased under a small speed from the value used in the constant rotational speed stage. If the rotational angular speed reaches to the value, above which although the rotational angular speed increases, the torque of motor almost does not change because slippage happens between sample and the lower blade. At this time, the measurement enters into Step 5.

Step 5: Rotational speed decreasing stage. The measurement is done under a decreasing rotational angular speed.

Step 6: Normal stress growth stage. If the rotational angular speed in the rotational speed decreasing stage is reduced to an extremely small value (about 5 deg./s). Keep the rotational angular speed constant, and the measurement is continued under the condition that the air pressure is adjusted at four levels (0 MPa, 0.3 MPa, 0.5 MPa, and 0.7 MPa).

Based on the measurement of Step 3~6, the shear stress τ_m, average shear strain rate $\dot{\gamma}_m$, and average normal stress σ_n of every stages are calculated. Then, the rheological parameters of Eq. (4) are obtained. Firstly, the relationship of $\tau_m-\dot{\gamma}_m$ in the rotational speed decreasing stage should be linear, as the down-curve shown in Figure 1(b), the slope of the line is determined as the essential viscosity η. Secondly, the linear relationship of $\tau_m-\sigma_n$ in the normal stress growth stage is plotted, then the ϕ is calculated according to the slope of the straight line. And the C_{w1} is calculated according to the stress difference between the stress at the intercept and $\eta\dot{\gamma}$. Thirdly, using the values of τ_f, σ_n and ϕ, C_{w1}, the average particle contact angle θ_f at shear failure point is calculated according to Eq. (3). Finally, using the experimental results of the constant rotational speed stage, the relational curve (straight line) of $\ln\{-\ln[(\tau_f-\tau)/\sigma_n\theta_f]\}-\dot{\gamma}(t-t_f)$ is plotted, followed by taking the slope of the straight line as κ.

4. TIME-DEPENDENCE OF RHEOLOGICAL PARAMETERS

4.1. Experiment

Based on the measuring methods explained above, the rheological parameters of the fresh concrete were measured at different elapsed times. The effective thickness of concrete sample, i.e. the height

Table 1. Mix proportions of concrete and the changes of fluidity with time

W/C	*s/a* (%)	Unit mass (kg/m^3)					Fluidity	Bulk density (kg/m^3)
		W	*C*	*S* (SD)	*G* (SD)	SP (*C*×%)		
0.38	44.6	165	434	748	980	1.5**	0min.: Sf. = 700 mm 60min.: *Sf.* = 450 mm, *Sl.* = 22cm 120 min.: *Sf.* = 300 mm, *Sl.* = 16 cm	2330

[Notes] *W/C*: Water-cement ratio by mass, *W*: Water, *C*: Ordinary Portland cement, *S*: Sea sand, *G*: Crushed stone, *s/a*: sand-aggregate ratio by volume, *Sl* : Slump, *Sf.*: Slump flow, SP: Retarding type water reducing agent.

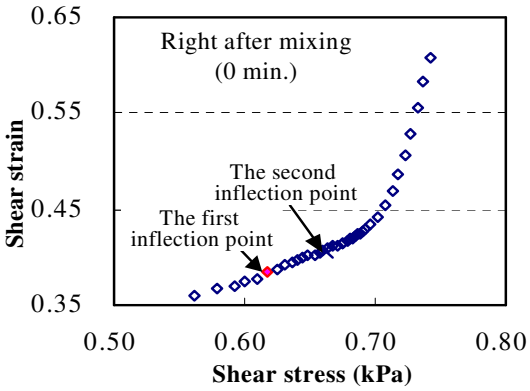

Figure 3. The γ_m~τ_m relationship before yield

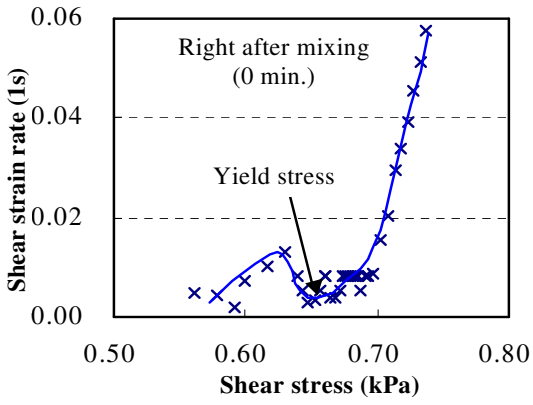

Figure 4. The γ_m~τ_m relationship before yield

between two blades was 100 mm. The mix proportions of the concrete are shown in Table 1. Sea sand, crushed stone, retarding type high-range water reducing agent were used. The measuring values of slump and slump flow at 0 min., 60 min. and 120 min. are also shown in Table 1.

The measurement was done by the RSNS rheometer at the three time points. The shear stress τ_m, average shear strain γ_m, and average shear strain rate $\dot{\gamma}_m$ were calculated respectively on basis of the basic information of motor torque, rotational angle, and rotational angle speed. The normal stress was also calculated by the gravity of concrete sample and round aluminum plate as well as vertical pressure of two air cylinders. Then, the parameters in Eqs.(1) and (2) were calculated.

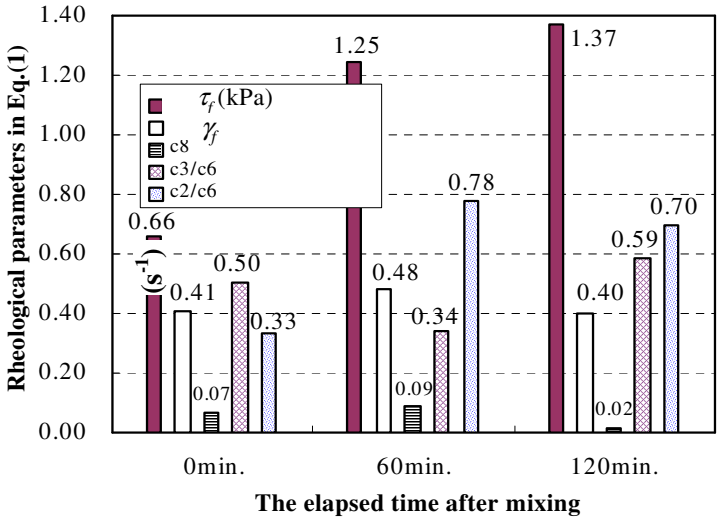

Figure 5. Measured values of the rheological parameters in Eq.(1) (Deformation model before yield)

4.2. Rheological parameters in Eq.(1)

The τ_m~γ_m relationship in the torque growth stage was obtained by the measurement of motor torque and rotational angle. As an example, the results measured immediately after mixing is shown in Figure 3. Because the torque increased after the constant torque stage, the relational curve does not

begin from zero stress. The shear stress and shear strain at the second reflection point on the $\tau_m \sim \gamma_m$ relational curve was taken as the shear stress τ_f and the shear strain γ_f at the shear failure point, respectively. The relationship of $\tau_m \sim \dot{\gamma}_m$ in the torque growth stage immediately after mixing is shown in Figure 4. The $\dot{\gamma}_m$ at the shear failure point is extremely small.

Figure 5 shows the relationship between the elapsed time and the τ_f, γ_f. With the elapsed time, the τ_f increased, whereas the γ_f did not almost change. The regressive analysis was done for the relationship between the logarithm of $(\tau_m/\sigma_n)/\gamma_m$ in the torque growth stage and the elapsed time t. According to the obtained regressive straight line, the c_2/c_6 and c_3/c_6 were calculated. The regressive analysis was also done for the relationship between the elapsed time and the logarithm of γ/γ_∞ obtained in the constant torque stage. Based on the slope of this relational line, the q was gotten, then the c_8 was further calculated. As shown in Figure 5, the longer the elapsed time after mixing, the larger the c_2/c_6 and c_3/c_6, but the smaller the c_8. One of the reasons of test error is that the fluidity of concrete sample after mixing was so high that segregation might happen near the lower blade.

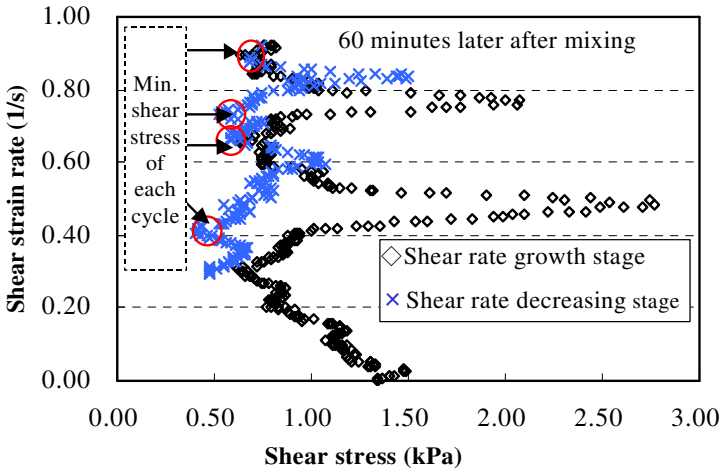

Figure 6. The $\dot{\gamma}_m - \tau_m$ relationships in the rotational speed growth stage and the rotational speed decreasing stage

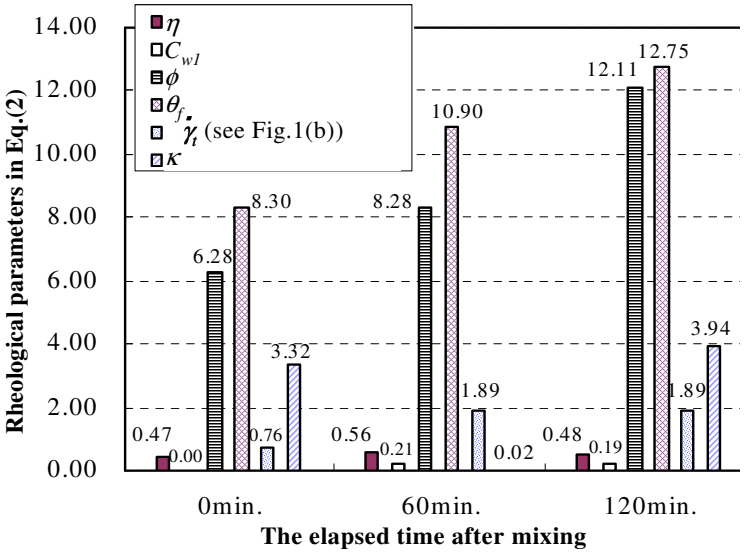

Figure 7. Measured values of the rheological parameters in Eq.(2) (Deformation resistance model after yield)

4.3. Rheological parameters in Eq.(2)

The $\tau_m \sim \dot{\gamma}_m$ relationships in the rotational speed growth stage and in the rotational speed decreasing stage were measured for the concrete sample at the three time points stated above. As an example, the experimental result at 60 min. is shown in Figure 6. At any of the stages, the shear stress did not always increase with the increase of shear strain rate, but changed in cycle of reduction-growth repeating. The shear stress also decreased with the increase of shear strain rate in the shear box test [11]. The repetition of reduction-growth-reduction of shear stress is due to sequentially strengthening and weakening of particle interlocking. The weakening is caused by shear flow, and the strengthening is caused by the restraint of the container's inside wall. In the beginning of the rotational speed growth stage, the shear strain rate was still small even if it was increased, and the increase in viscous resistance with shear rate was limited, thus the decrease in shear resistance due to the weakening of particle interlocking was dominant so that even if the shear strain rate was increased, the shear stress

still decreased. In theory, once particles are dispersed, it is considered that particle flocculation or particle interlocking can not be reformed provided that shear flow continues. However, since the moving field of particle is limited by the box or the skirt, the particle interlocking reforms with the deformation of sample even after the sample entered in the failure state. Because of the strengthening of particle interlocking, shear resistance and shear stress increase. If the reformed particle interlocking is destroyed by sample flow, the shear resistance decreases again.

Based on the regressive analyses of the relationships between the shear rate and the minimum shear stress of each reduction–growth repeating cycle on the down-curve measured at three time points, the essential viscosities at three time points were gotten. Moreover, in the normal stress growth stage, at which the shear rate was a constant, the shear stress under the same normal stress changed with time t in a cycle of reduction-growth repeating. The regressive analysis was done for the relationship between normal stress and the minimum shear stress of each cycle of reduction-growth repeating measured right after the air pressure of cylinders was changed. The ϕ and C_{w1} were calculated on basis of this regressive analysis. Using the shear stress in the constant rotational speed stage, the relational curve (straight line) of $\ln\{-\ln[(\tau_f - \tau)/\sigma_n\theta_f]\}$ and $\dot{\gamma}(t-t_f)$ is plotted, and κ is gotten, which is the slope of the straight line.

As shown in Figure 7, the longer the elapsed time after mixing fresh concrete, the larger the ϕ, θ_f and $\dot{\gamma}_f$. However, although the essential viscosity η and the parameter C_{w1} increased with the elapsed time, but they tended to decrease when the elapsed time was continuously increased. The κ showed an opposite tendency to the essential viscosity η.

5. SUMMARY

This paper firstly introduced the VGM model as shown in Eqs.(1) and (2), which is applied to viscous granular materials, and can describe the nonlinear feature, pressure-dependence, and thixotropy of deformation and flow behaviors of fresh concrete. For measuring the parameters in the VGM model, the authors developed a ring shear test device (called RSNS rheometer) controlled by whether torque control method or rotational speed control method, and the test methods of the rheological parameters were further proposed. Finally, the rheological parameters of high fluidity concrete were measured by the RSNS rheometer, and their changes over standing time were discussed.

According to the experimental results that the rheological parameters of high fluidity concrete changed over standing time, with the increase of the standing time, the τ_f, ϕ, θ_f, $\dot{\gamma}_f$, c_2/c_6 and c_3/c_6 became large, but the γ_f almost did not change, and the c_8 decreased. Moreover, the η and the C_{w1} increased with the elapsed standing time, but they decreased on the contrary if the elapsed time was too long. The time-dependence of the κ is opposite to the η and the C_{w1}.

REFERENCES

[1] Tattersall G. H. (1973). The rational of a Two-Point workability test, *Magazine of Concrete Research*, 25 (84), 169-172.

[2] Mori H., Tanaka M. and tanigawa Y. (1991). Experimetnal strudy on the shear deformation of fresh concrete, *Journal of Structural and Construction Engineering* (Transaction of AIJ), 421, 1-10 (in Japanese).

[3] Larrrd F. de, Ferraris C. F., and Sedran T. (1998). Fresh concrete: a Herschel-Bukley material, *Material and Structure*, 31(211), 494- 498.

[4] Roussel N. (2006). A thixotropy model for fresh fluid concretes: Theory, validation and applications, *Cement and Concrete Research*, 36, 1797-1806.

[5] Wallevik O. H., and Gjorv O. E. (1990). Development of a Coaxial Cylinder Viscometer for Fresh Concrete, *Proceedings of the RILEM Colloquium*, Hanover, 213-224.

[6] Larrard F. D., and Hu C., et al. (1997). A new rheometer for soft-to-fluid fresh concrete, *ACI Materials Journal*, 94(3), 234-243.

[7] Beaupre D., and Mindness S. (1994). Rheology of fresh shotcrete, *Proceedings of Special Concretes: Workability and Mixing* (Scotland), 225-235.

[8] Tattersall G. H., and Bloomer S.J. (1979). Further development of the Two-Point test for workability and extension of its range, *Magazine of Concrete Research*, 31, 202-210.

[9] Koehler E.P., and Fowler D.W. (2004). Development of a portable rheometer for fresh portland cement concrete, *Report of International Center for Aggregates Research*, The University of Texas at Austin (No.: ICAR105-3F), 57-176.

[10] Ukraincik V. (1980). Study on fresh concrete flow curves, *Cement and Concrete Research*, 10, 203-212.

[11] Mishima N. (2001). Reological model of dense suspension in consideration of dilatancy and particle flocculation, *Ph. D. thesis of Nagoya University*, 84-94 (in Japanese).

[12] Li Z., TanigawaY., Mori H., and Kurogawa Y. (1999). Study on rheological constitutive law of fresh mortar using particle assembly model, *Journal of Structural and construction Engineering* (Transactions of AIJ), 523, 17-24(in Japanese).

[13] Li Z., Tanigawa Y., Mori H., and Ohkubo T. (2001). Study on limit stress at shear failure of fresh mortar by microscopic approach, *Journal of Structural and construction Engineering* (Transactions of AIJ), 542, 47-53(in Japanese).

[14] Li Z., and Li J. (2010). Experimental investigation on shear deformation of fresh concrete, *Journal of Structural and construction Engineering* (Transactions of AIJ), 75(653), 1173-1180 (in Japanese).

[15] Li Z. (2013). Theoretical investigation on the rheological properties of fresh concrete, *Journal of Structural and construction Engineering* (Transactions of AIJ), 78(687), 895-904 (in Japanese).

[16]Li Z., Li J., and Iidaka, M. (2011). Development of stress-controlled rheometer for fresh concrete, *Proceedings of the Japan Concrete Institute*, 33(1), 1211-1216 (in Japanese).

[17] Li Z. (2015). Study on rheological model and rheometer of fresh concrete, *Journal of Structural and construction Engineering* (Transactions of AIJ), 80(710), 527-537(in Japanese).

[18] Hu C., and Larrard F. D., et al. (1996). Validation of BTRHEOM, the new rheometer for solid-to-fluid concrete, *Materials and Structure*, 29, 620-631.

[19] Hu, C. (1995). Rheology of fluid concretes", *Ph. D. thesis of ENPC*, l~tudes et P, echerches des LPC, S&ie ouvrages d'art (in France)

[20] Sadrekarimi A., and Olson S. M. (2011). A new ring shear device to measure the large displacement shearing behavior of sands, *Geotechnical Testing Journal*, 32(3), 1-12.